12^{th} International Conference on Fracture Mechanics of Concrete and Concrete Structures
FraMCoS-12
B.L.A. Pichler, Ch. Hellmich, P. Preinstorfer (Eds)

https://doi.org/10.21012/FC12.1255
TT-C2:1

NUMERICAL STUDY OF BRAZILIAN TESTS OF UHPFRC BY USING ELEMENTS WITH EMBEDDED COHESIVE CRACK AND COHESIVE JOINT ELEMENTS

BEATRIZ SANZ*, JAIME PLANAS† AND JOSÉ M. SANCHO‡

* Universidad Politécnica de Madrid, ETSI Caminos, Canales y Puertos, Profesor Aranguren 3, Madrid, Spain
e-mail: beatriz.sanz@upm.es

† Universidad Politécnica de Madrid, ETSI Caminos, Canales y Puertos, Profesor Aranguren 3, Madrid, Spain
e-mail: jaime.planas@upm.es

‡ Universidad Politécnica de Madrid, ETSI Caminos, Canales y Puertos, Profesor Aranguren 3, Madrid, Spain
e-mail: jose.sancho@upm.es

Key words: Cohesive Crack, Diametral Compression Tests, Fiber Reinforced Concrete, Quasi-brittle Material, Finite Element Method

Abstract. Ultra-high performance fibre-reinforced concrete (UHPFRC) is an emergent material with outstanding mechanical properties which still needs research regarding the characterisation and modelling of its fracture behaviour. The present work focusses on the determination of the tensile strength, conceived as the stress corresponding to crack initiation. The Brazilian test is a convenient experimental option in the case of plain concrete which provides a sufficient accurate value of the tensile strength obtained from the maximum load of the test, provided that it is performed with the adequate conditions of geometry and load rate, because the peak load occurs very soon after crack initiation. However, in the case of fibre-reinforced materials, the peak load can occur much after crack initiation and so the apparent splitting strength be much higher than the true tensile strength. Nevertheless, in previous experimental and numerical works it has been assessed that a local maximum occurs in many cases at a splitting stress close to the tensile strength of the material. It means that the stress corresponding to initiation of cracking can be determined in Brazilian tests provided that the test is properly designed and instrumented taking into account the size-effect to ensure detection of the local maximum. As shown in a previous numerical study, numerical simulations are an essential tool for this purpose; however, a systematic parametric study is still necessary. The current work analyses the main alternatives for dimensionless simulations within the finite element framework COFE (Continuum Oriented Finite Element). In this study, the results of simulations of the Brazilian tests by considering a domain in which all the elements can crack are compared with those obtained by using joint elements with a cohesive behaviour along of the foreseeable cracking plane, and the main aspects of the dimensionless simulations are analysed in detail.

1 INTRODUCTION

Ultra-high performance fibre-reinforced concrete (UHPFRC) is an emergent material with outstanding mechanical properties, as for example a compressive strength several times that of ordinary concrete, due to special formulations which lead to very high compact mixtures [1, 2]. It presents a high technological interest, but still needs research regarding char-

acterisation and modelling of its fracture behaviour. Specifically, this work focusses on the determination of the tensile strength, conceived as the stress corresponding to crack initiation.

As an alternative to the direct tensile tests, in previous works of the Authors it was proposed that a version of the diagonal compression splitting tests, also known as the *Brazilian test*, with the adequate instrumentation is used, due to the advantage of its clear boundary conditions and easy execution [3,4]. The sound version of this experiment has been widely used for ordinary concrete and other quasi-brittle materials, as it provides a sufficiently accurate value of the tensile strength if the test is performed with the appropriate conditions of loading rate and width of the bearing strip bands [5,6]. In the case of fibre-reinforced materials, the peak load of the test may occur for a stress much higher than that of crack initiation due to the test configuration and to the bridging effect of fibres, and, hence, the tensile strength cannot be determined from the record of maximum load. However, a local maximum occurs close to the tensile strength, as assessed in previous numerical studies, which can be detected if the test is adequately instrumented [3] and determined with enough accuracy if the test is properly designed taking into account the effect of the size and material properties [7]. In the previous work, three ratios between the specimen size and a material characteristic length together with seven softening curves were considered, but other values of those should be considered.

Moreover, in a different context of an experimental study carried out in collaboration with the Spanish Association of Railway Sleeper Element Manufacturers [8], whose main objective was to determine the brittleness length of concrete in factories by using a particular implementation of an existing method and provide experimental verification of that [9], it was found that the size-effect curves of the Brazilian test of quasi-brittle materials should be enlarged, since some new mixtures used in the factories present values out of the ranges considered in [10].

Both cases call for a systematic parametric study, whose basis are analysed in the current work. In particular, the current work analyses the main alternatives for dimensionless simulations within the finite element framework COFE (Continuum Oriented Finite Element) in which elements with a cohesive embedded crack are used [11]. In particular, the results of simulations of the Brazilian tests of cylindric specimens by considering a domain in which all the elements can crack are compared with those obtained by using joint elements with a cohesive behaviour along the foreseeable cracking plane in the case of linear softening, in order to select the best option for a further parametric study, and the main aspects of the dimensionless simulations are analysed.

In the paper, following to this introduction, Section 2 overviews the model for the fracture behaviour of concrete, the basis of the dimensionless simulations and the parameters used in this work, Section 3 analyses and discusses the results and Section 4 presents the main conclusions.

2 NUMERICAL SIMULATIONS

The basis of the simulations are those reported in [3] and are summarised next for completeness of the text.

2.1 Theoretical background

For the fracture behaviour of concrete, a generalisation of the cohesive crack model was used, which follows the main principles introduced by Hillerborg et al [12]. In particular, it is assumed that when a crack develops in Mode I, it still transmits stress σ across its faces following a unique relation $f(w)$ which depends on the crack width w, which is called the *softening curve*. For general loading, a vectorial traction-separation law is assumed considering the traction vector $\mathbf{t}$ acting on one of the faces of the crack and the crack separation vector $\mathbf{w}$. In this work, the damage-based vectorial model proposed in [13] has been used, which considers the ratio between the fracture energies in modes II and I α^2 and the ratio between the

shear and normal stiffnesses β^2 through the following vectorial law:

$$\mathbf{t} = \frac{f(\kappa)}{\kappa}(w_n\mathbf{n} + \beta^2\mathbf{w}_s), \qquad \kappa = \max[w^{eq}(\mathbf{w})] \tag{1}$$

where w_n and $\mathbf{w}_s$ are the normal and shear components of the displacement vector, respectively, which are calculated as $w_n = \mathbf{w}\cdot\mathbf{n}$ and $\mathbf{w}_s = \mathbf{w} - w_n\mathbf{n}$, with $\mathbf{n}$ the unit normal of the reference face of the crack, and κ a damage variable which is computed as the maximum value of an equivalent separation w^{eq}. This parameter is defined together with an equivalent traction t^{eq} as

$$w^{eq} := \sqrt{w_n^2 + \frac{\beta^2}{\alpha^2}w_s^2}, \qquad t^{eq} := \sqrt{t_n^2 + \frac{t_s^2}{\alpha^2\beta^2}} \tag{2}$$

where w_s is the modulus of the shear component of the displacement vector, and t_n and t_s the moduli of the normal and the shear components of the traction vector, respectively, which are computed analogously to w_n and w_s. In this work we assume $\alpha = \beta = 1.0$, according to the results reported in [13].

In this work a linear softening curve has been used to reproduce the fracture behaviour of concrete, which is defined by the tensile strength f_t and the horizontal intercept with the abscissas axis w_1.

The simulations of this work have been carried out within the finite element framework COFE (*Continuum Oriented Finite Element*, which implements elements with an embedded adaptable crack [11, 14]. In those, the crack is allowed to changed its direction until a given threshold width $w_{th} = \alpha' w_1$ is reached, where $\alpha' = 0.2$ is the adaptation factor.

Dimensionless simulations have been carried out, according to the basis explained in [15], by considering a dimensionless softening function $\hat{f}$:

$$\sigma = f(w) = f_t\hat{f}\left(\frac{w}{w_1}\right) . \tag{3}$$

where f_t and w_1 are the parameters that define the linear softening curve, as explained before. It means that all the values of stress σ are divided by f_t, and the values of displacement and crack separation w are divided by w_1. In coherence, dimensionless geometrical lengths are considered by dividing all the values by the specimen diameter D. As a result, the elastic modulus of linear elastic materials is scaled and results in:

$$E^* = \frac{\ell_2}{D}, \quad \ell_2 := \frac{Ew_1}{f_t} \tag{4}$$

where l_2 is a brittleness length of the material which we call the *second brittleness length*, and is related to the brittleness length l_1 used in other works [5, 9] as $l_2 = 2l_1$.

Since the size-effect is analysed by modifying the ratio l_1/D as in [5, 10], and this can be achieved by modifying the diameter or any of the parameters that define l_2, the option adopted in this work has been to maintain the specimen size D, the tensile strength f_t and the horizontal intercept w_1, while varying the elastic modulus E accordingly through the dimensionless modulus E^*. Note that an increase in the ratio l_2/D is equivalent to diminish the size of the specimen or to consider a less brittle material.

2.2 Parameters of the simulations

As mentioned in the previous section, linear softening has been considered in the current simulations, although bilinear curves will be considered in further studies as in [7] to simulate the effect of fibres. The parameters that define the linear curve —dimensionless tensile strength and dimensionless horizontal intercept— have been maintained constant and equal to 1.0. The uncracked material is modelled as linear elastic, with Poisson's ratio $nu = 0.17$ and a scaled elastic modulus E^* variable as the driving parameter in this study. Table 2.2 displays its values and the equivalent ratios to be compared with those used in the literature [10].

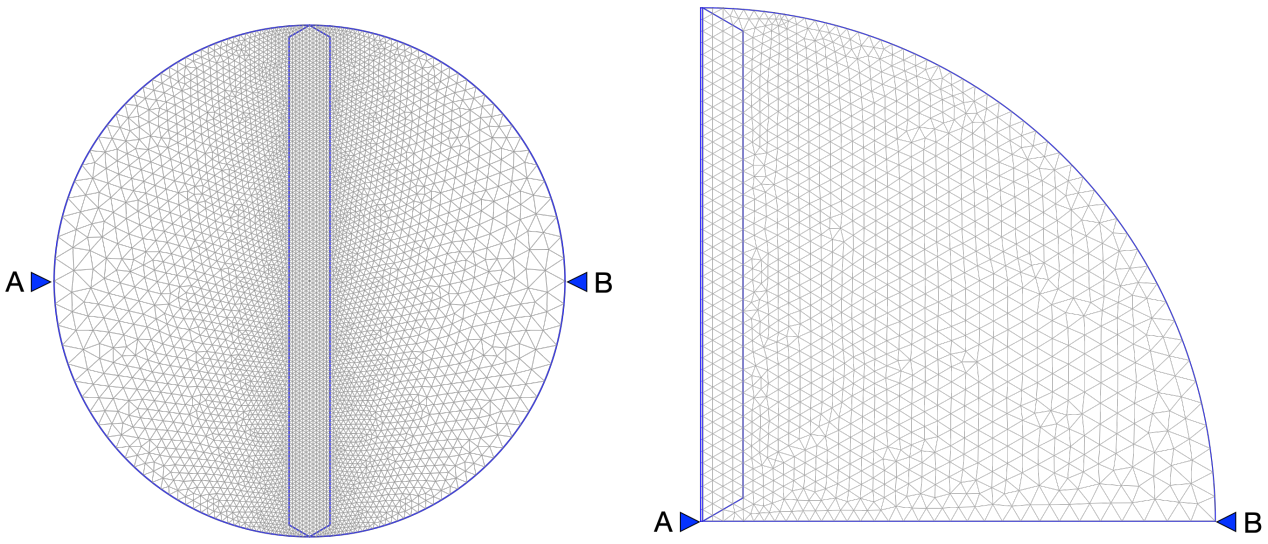

(a) (b)

Figure 1: Models used in this study: complete cylindric specimens (a) and quarter of cylinders with a layer of joint elements (b).

Table 1: Parameters in the simulations: dimensionless elastic modulus E^* and ratio between the specimen diameter and the brittleness length D/l_1.

E^*	1.0	2.0	4.0	8.0	16.0
D/l_1	2.0	1.0	0.5	0.25	0.125

Two types of bi-dimensional models have been used, both with dimensionless diameter equal to 1.0: (a) complete cylindric specimens in which all elements can crack and (b) quarter of cylinders with a layer of joint elements at the foreseeable cracking plane. Figure 1 shows a sketch of the definition of the two models. In both cases the width of the loading band was $b = 0.08D$ as in [7], but other values will be considered in further works for the enlargement of the size-effect curves provided in [10].

The mesh was generated using the program Gmsh [16] with the meshing algorithm set to "Delauny". In the complete cylinder, two zones were defined for meshing, delimited by the blue lines that are seen in Fig. 1: in the central part, where the main crack is expected to develop, the mesh was finer and structured in order to capture the crack path and ensure adequate element shape; in the remaining zones, the mesh was unstructured and the size of elements was enlarged up to seven times that of the central part at the right and left outer nodes. The number of elements over the half-loading strip was six, and the size and refinement of the structured zone coincided with that of the bearing bands. The two zones were meshed with constant strain triangles (CST) with a cohesive embedded crack. The mesh has 5557 nodes and 10970 elements. In the quarter cylinder, two zones of CST with a cohesive embedded crack were defined as well, structured and unstructured, with the same purpose as in the complete cylinders. The shape of the central zone was selected to ensure be filled with equilateral triangles. The mesh was prepared to consider other widths of the bearing band without altering its definition, which causes the number of elements in the loading strip to be multiple of 4.0 and the element size constant in the outer boundary up to $0.08D$. Particularly, the number of elements over the half-loading strip in the current work was set to the minimum, 4.0, which is enough accurate for the purpose of validation of the models, according to the results presented in Sec. 3, but simulations with a greater number will be performed to increase precision of the extended size-effect curves. To speed up the computations, a layer of joint elements was placed at the foreseeable

cracking plane with a cohesive behaviour. Note than in the joint elements, the input parameters of the softening curve were equivalent to those of the triangles, which implies that the horizontal intercept is 0.5 due to the symmetry. In addition, the joint elements use a penalty stiffness whose value was selected as $10^{3.5}$ to have an error in the nominal stress less than $0.05\% f_t$. The mesh has 1366 nodes and 2744 elements.

A uniform stress was applied at two lines of nodes situated at the outer boundary of the specimen that simulate the bearing strips of the experiments, as a uniform stress vector in the case of the complete cylinders and as the application of a uniform stress tensor in the case of the quarter cylinders. The simulations were driven by the horizontal displacement between the nodes labeled as A and B in Fig.1, in order to obtain stable calculations. For the complete cylinders, a given total displacement was applied in steps with three different magnitudes in order to capture the maximum or the stress near the tensile strength with enough resolution. For the quarter cylinders, the displacement was applied in steps with seven different magnitudes.

3 RESULTS

From the recorded load P, the nominal stress σ_N was computed, according to the formula of the ASTM-C496 standard [17], as:

$$\sigma_N = \frac{2P}{\pi DL} \tag{5}$$

where D is the specimen diameter and L the specimen length. In the figures, the dimensionless nominal stress σ_N / f_t is displayed.

Figure 2 shows the dimensionless curves of nominal stress versus horizontal displacement and the curves of nominal stress versus maximum crack width for the complete cylindric specimens, which show equivalent results except for the elastic contribution of the material. Figure 3 shows the same curves for the quarter of cylinders with a layer of joint elements. For the two models, a marked peak was obtained for the curves corresponding to l_2/D equal to 1.0 and 2.0 with a value very close to the tensile strength of the model, but as l_2/D increases, the peak smoothes and the load corresponding to the peak is greater, in coherence with the results shown in [10].

Figure 4 shows the dimensionless tensile splitting strength f_{ts}/f_t versus the ratio D/l_1 for the two models, showing a significant error in the estimation of the tensile strength for the lowest ratio D/l_1, which corresponds to $l_2/D = 16.0$, i.e., the less brittle behaviour, which calls for updated analytical expressions of the size-effect curves in order to correct the value of the tensile strength obtained from the Brazilian tests and reduce the error.

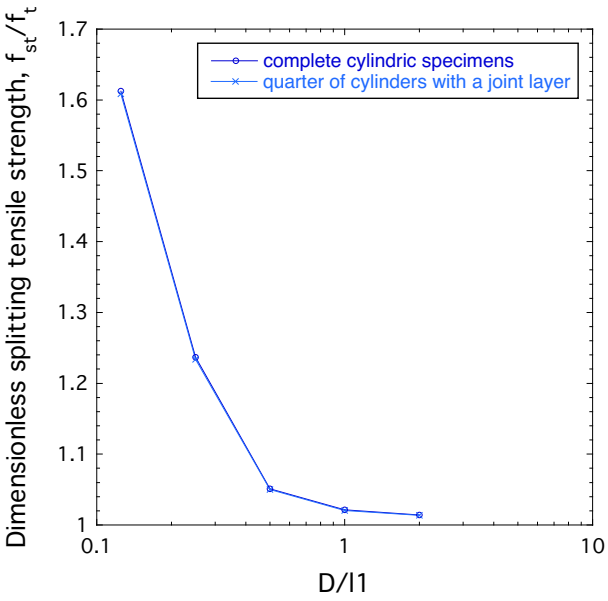

Figure 4: Dimensionless tensile splitting strength f_{ts}/f_t versus the ratio D/l_1 for complete cylinders and quarter cylinders with a layer of elements.

The particular values of the dimensionless tensile splitting strength obtained for each model and the difference between both referred to the result of the complete cylinders are displayed in Table 3, showing that both methods provide sufficiently close results. It can be observed that the greatest difference was found for l_2/D equal to 8.0 and 16.0, in which precisely the steps were refined near the tensile strength instead of near the maximum, which means that the result of splitting tensile strength could be improved.

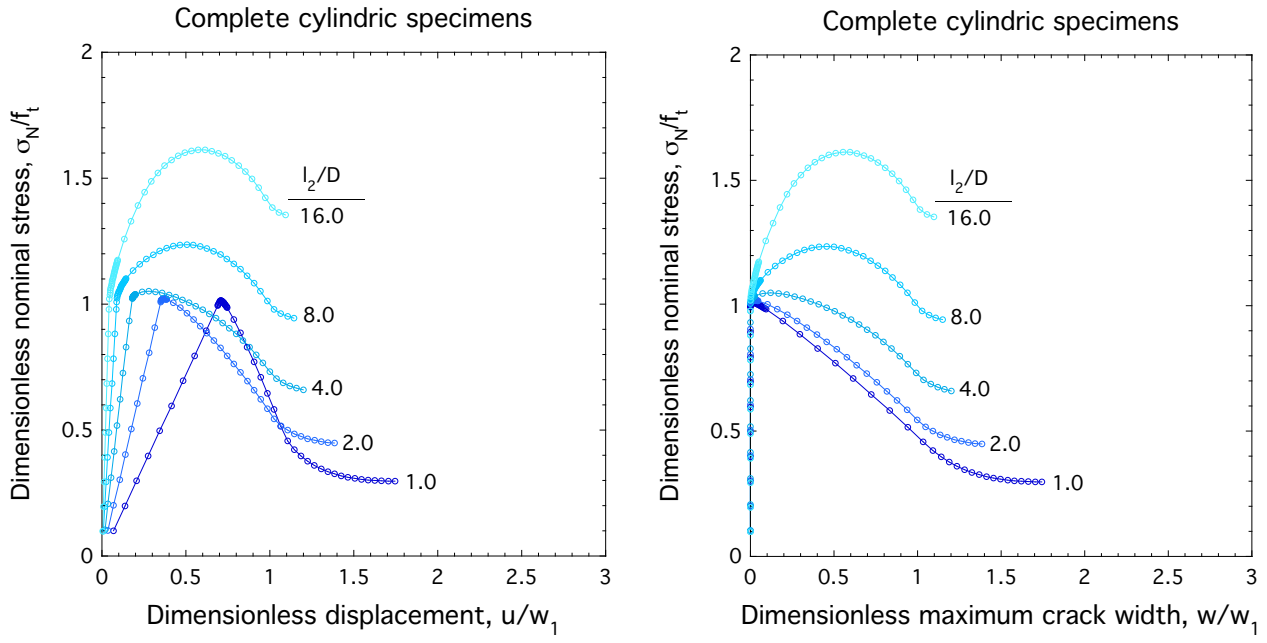

(a) (b)

Figure 2: Results of complete cylindric specimens: dimensionless curves of nominal stress versus horizontal displacement (a) and dimensionless curves of nominal stress versus maximum crack width (b) for values of l_2/D ranging from 1.0 to 16.0.

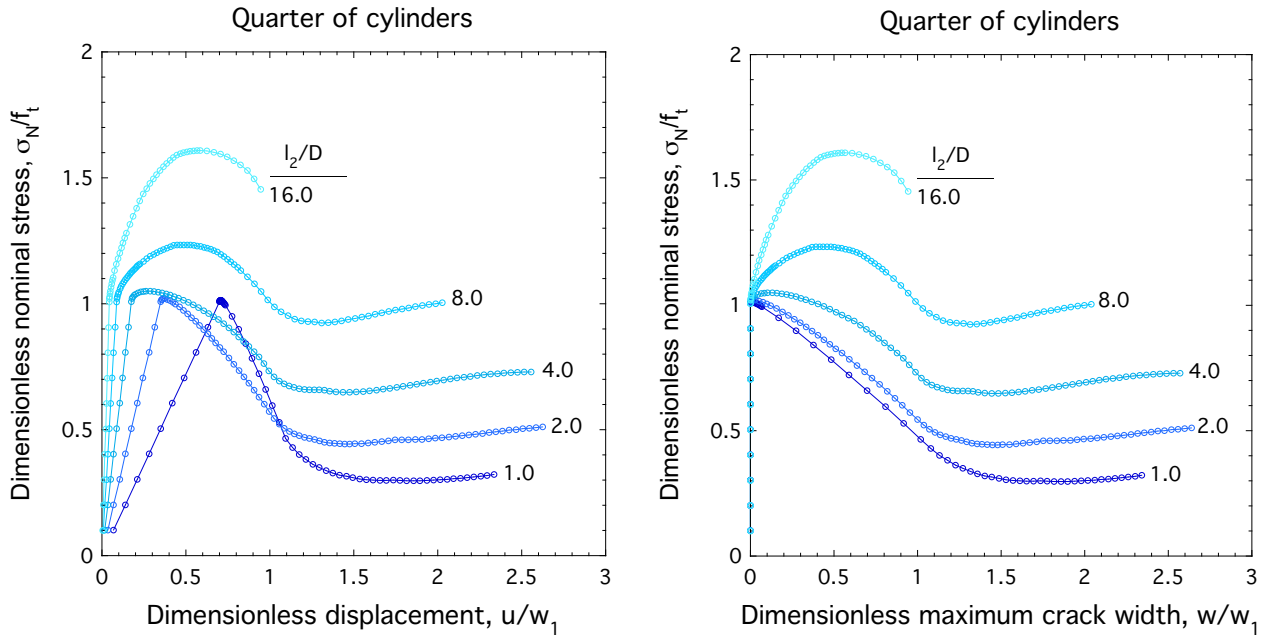

(a) (b)

Figure 3: Results of quarters of cylinders with a layer of joint elements: dimensionless curves of nominal stress versus horizontal displacement (a) and dimensionless curves of nominal stress versus maximum crack width (b) for values of l_2/D ranging from 1.0 to 16.0.

Table 2: Parameters in the simulations: dimensionless elastic modulus E^* and ratio between the specimen diameter and the brittleness length D/l_1.

D/l_1	2.0	1.0	0.5	0.25	0.125
Complete cyls.	1.014	1.0212	1.0512	1.2365	1.6124
Quarter cyls.	1.013	1.0203	1.0500	1.2339	1.6088
Difference (%)	0.0515	0.0907	0.109	0.211	0.228

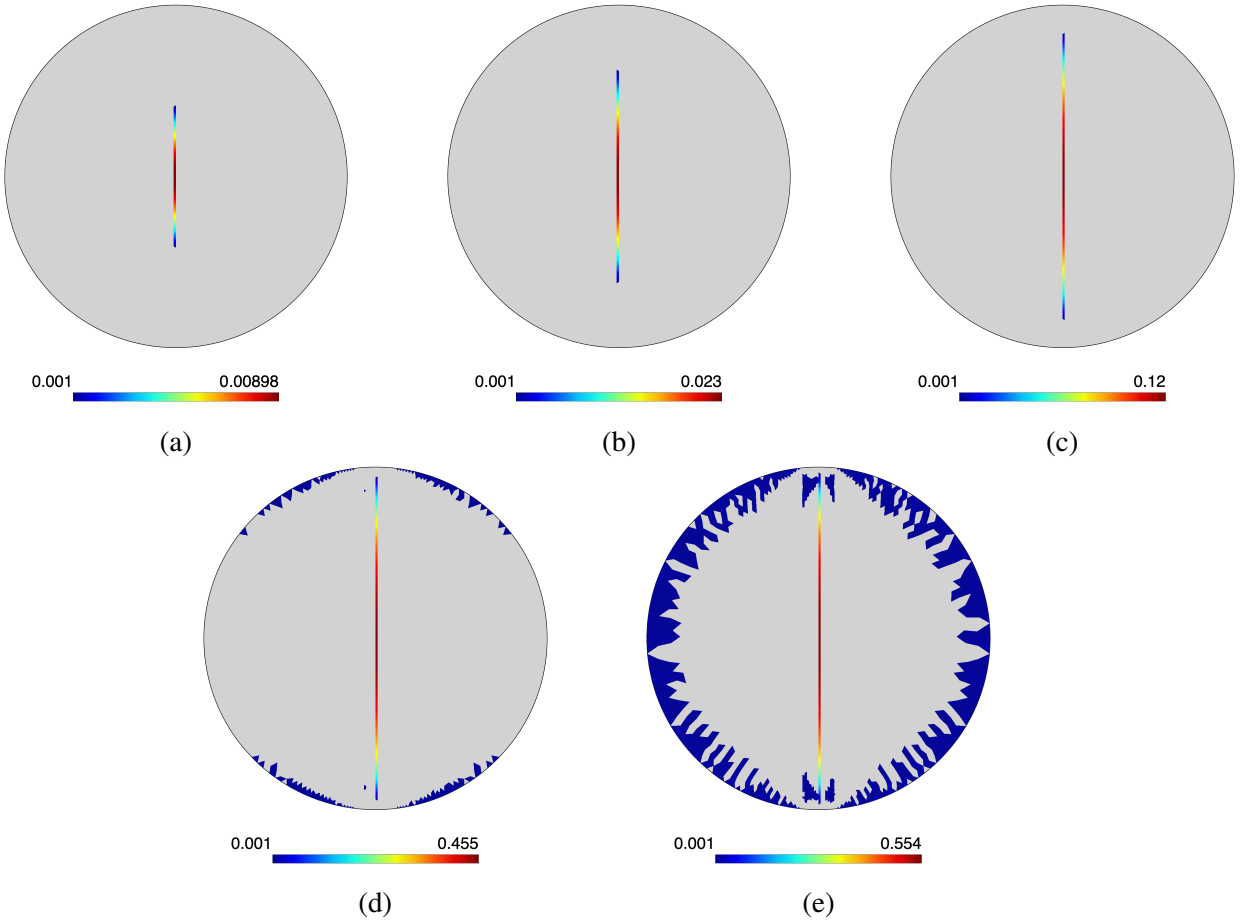

Figure 5: Crack pattern obtained at the peak load for values of the ratio l_2/D equal to 1.0 (a), 2.0 (b), 4.0 (c), 8.0 (d) and 16.0 (e), where the scale displays the dimensionless crack width, w/w_1.

For completeness, the crack pattern obtained at the peak load is displayed in Fig. 5 for the complete cylindric specimens, with the scale displaying the dimensionless width of the crack. It is observed that in all cases a main crack develops from the centre of the specimen to the outer boundary. It is remarkable that secondary cracking is predicted for the specimens with $l2/D$ equal to 8.0 and 16.0, in contrast with the more brittle specimens.

Finally, the influence of the mesh size in the quarter cylinders with a layer of joint elements and $l_2/D = 1.0$ is shown in Figure 6, for meshes with 4, 8, 12 and 16 elements in the half-loading strip (with 1366, 3255, 5597 and 8378 nodes, respectively). As shown in Fig. 6(a), almost coinciding dimensionless curves of nominal stress versus displacement and versus crack opening were obtained for the four meshes. However, if the curves are zoomed in the peak, as shown in Fig. 6(b), it can be observed a slight difference in the curve with 4 elements, which should be considered for the obtention of precise size-effect curves. Note that some of the steps of the mesh with 16 elements did not converge, so the corresponding data should be considered with restrictions.

4 CONCLUSIONS

A numerical analysis of the Brazilian test has been carried out for complete cylindric specimens and for quarter cylinders with a joint layer along of the foreseeable cracking plane, showing the validity of both models, as the main conclusion of this work. In particular, values of the ratio between a given material characteristic length and the specimen diameter l_2/D ranging from 1.0 to 16.0 and linear softening have been considered, but note that further simulations are necessary to complete the size-effect curves of concrete according to the parameters of the new mixtures and to investigate the local maximum of fibre-reinforced materials.

Other partial conclusions are drawn as follows:

- A marked peak is obtained close to the tensile strength for brittle specimens, but it smoothes and increases its value as l_2/D increases, in coherence with the results reported in [10], and leading to a significant error in the cases with $l_2/D \geq 8.0$. Updated expressions of the size-effect curves should be obtained in oder to correct the value with enough accuracy in those cases.
- The results obtained from the complete cylindric specimens and the quarter cylinders with a layer of joint elements are very close, with a difference less than 0.228% in the determination of the tensile splitting strength in the worst situation.
- The mesh size has a small influence on the peak of the quarter cylinders for the considered values, but meshes with eight elements in the half-loading strip are preferred to obtain precise size-effect curves.

ACKNOWLEDGEMENTS

The authors gratefully acknowledge the financial support received for this work under grant PID2021-125553NB-I00 from MCIN/AEI/10.13039/501100011033/FEDER, UE.

REFERENCES

[1] Roy, D., Gouda, G., and Bobrowsky, A., 1972. Very high strength cement pastes prepared by hot-pressing and other high-pressure techniques. *Cement and Concrete Research* **2**:349–366.

[2] Yudenfreund, M., Odler, I., and Brunauer, S., 1972. Hardened portland cement pastes of low porosity i. materials and experimental methods. *Cement and Concrete Research* **2**:313 – 330.

[3] Sanz, B., Planas, J., Rey de Pedraza, V., Sancho, R., Sancho, J.M., and Gálvez, F., 2022. Numerical and experimental study of initiation of cracking of uhpfrc by means of brazilian tests. *Theoretical and Applied Fracture Mechanics* .

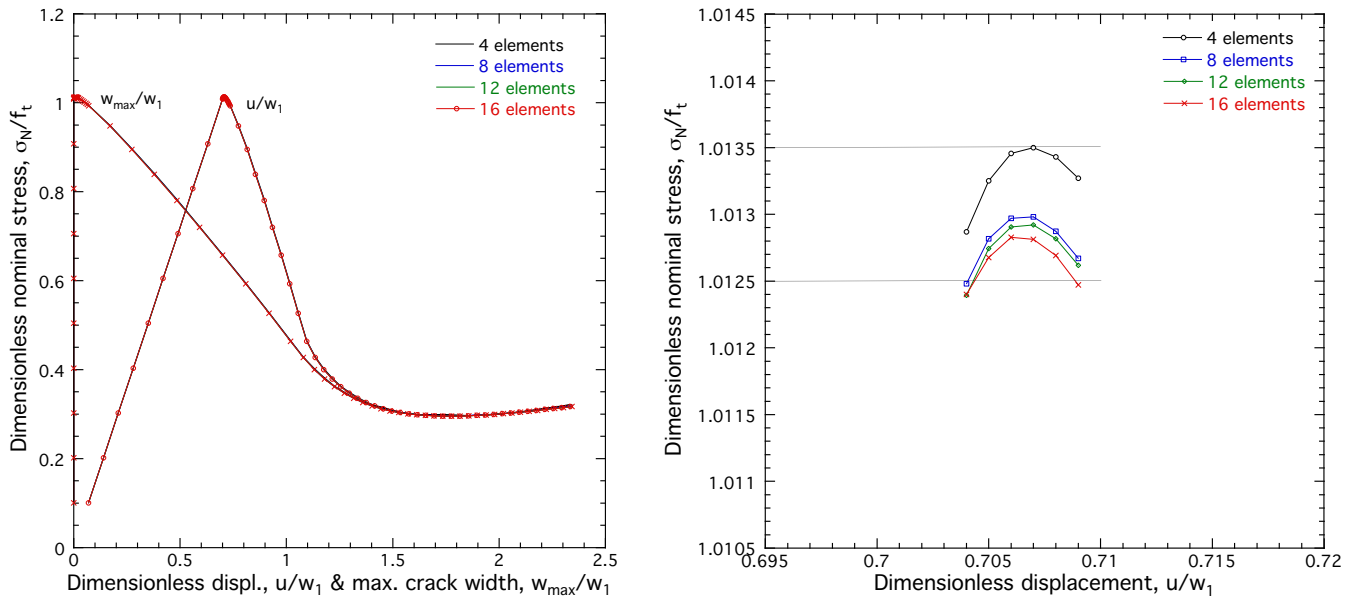

(a) (b)

Figure 6: Influence of the mesh size in the quarter cylinders with a layer of joint elements: dimensionless curves of nominal stress versus horizontal displacement and versus maximum crack width (a), and zoom in the peak of the curves of nominal stress versus horizontal displacement, for meshes with 4, 8, 12 and 16 elements over the half-loading strip.

[4] Sanz, B., Planas, J., Rey de Pedraza, V., Sancho, R., Sanz, J., Sancho, J., and Gálvez, F., 2021. Experimental and numerical analysis of brazilian tests in the determination of the tensile strength of uhpfrc. *Revista de Mecánica de la Fractura* **2**:41–46.

[5] Rocco, C., Guinea, G.V., Planas, J., and Elices, M., 1999. Mechanisms of rupture in splitting test. *ACI Materials Journal* **96**:52–60.

[6] Rocco, C., Guinea, G.V., Planas, J., and Elices, M., 1999. Size effect and boundary conditions in the brazilian test: Experimental verification. *Materials and Structures* **32**:210–217.

[7] Sanz, B., Planas, J., and Sancho, J.M., 2022. Simulation of brazilian tests of ultra-high performance fibre-reinforced concrete, in *Computational Modelling of Concrete and Concrete Structures*, pp. 130–137.

[8] Sanz, B., Planas, J., and Albajar, L., 2022. Experimental verification of indirect tests for stress-crack opening curve of concrete in tension from a round robin test: application to railway sleeper elements. *Materials and Structures* **55**:217.

[9] Planas, J., Guinea, G.V., Gálvez, J.C., Sanz, B., and Fathy, A.M., 2007. Chapter 3. indirect tests for stress-crack opening curve, in J. Planas (Ed.), *Report 39: Experimental Determination of the Stress-Crack Opening Curve for Concrete in Tension - Final report of RILEM Technical Committee TC 187-SOC*, pp. 13–29, RILEM Publications SARL.

[10] Rocco, C., Guinea, G.V., Planas, J., and Elices, M., 1999. Size effect and boundary conditions in the brazilian test: Theoretical analysis. *Materials and Structures* **32**:437–444.

[11] Sancho, J.M., Planas, J., Cendón, D.A., Reyes, E., and Gálvez, J.C., 2007. An embedded crack model for finite element analysis of concrete fracture. *Engineering Fracture Mechanics* **74**:75–86.

[12] Hillerborg, A., Modéer, M., and Petersson, P.E., 1976. Analysis of crack formation and crack growth in concrete by means of fracture mechanics and finite elements. *Cement and Concrete Research* **6**:773–781.

[13] Planas, J., Sanz, B., and Sancho, J., 2020. Vectorial stress-separation laws for cohesive cracking: in concrete and other quasibrittle materials. *International Journal of Fracture* **223**.

[14] Sancho, J., Planas, J., Fathy, A.M., Gálvez, J.C., and Cendón, D., 2007. Three-dimensional simulation of concrete fracture using embedded crack elements without enforcing crack path continuity. *International Journal for Numerical and Analytical Methods in Geomechanics* **31**:173–187.

[15] Planas, J., Sanz, B., and Sancho, J., 2021. Numerical analysis of size-effect in uhpfrc beams subjected to wide-span four-point bending. *Revista de Mecánica de la Fractura* **1**:149–154.

[16] Geuzaine, C. and Remacle, J.F., 2009. Gmsh: A 3-d finite element mesh generator with built-in pre- and post-processing facilities. *International Journal for Numerical Methods in Engineering* **79**:1309–1331.

[17] ASTM-C496, 1990. *Standard Test Method for Splitting Tensile Strength of Cylindrical Concrete Specimens*, Technical report.